

On the detection of pre-low-mass X-ray binaries

B. Willems* and U. Kolb*

Department of Physics and Astronomy, The Open University, Walton Hall, Milton Keynes, MK7 6AA, UK

Accepted ... Received ...; in original form ...

ABSTRACT

We explore the population of candidate pre-low-mass X-ray binaries in which a neutron star accretes mass from the wind of a low-mass companion (mass $\leq 2 M_{\odot}$) in the framework of a binary population synthesis study. The simulated accretion-luminosity distribution shows a primary peak close to 10^{31} erg/s and a secondary peak near 10^{28} erg/s. The relative contribution of the two peaks depends primarily on the magnitude of the kick velocity imparted to the neutron star at birth. The secondary peak is negligible for average kick velocities larger than ~ 200 km/s, but becomes dominant for average kick velocities smaller than ~ 50 km/s. Regardless of the relative contributions of the two peaks, our calculations suggest that pre-low-mass X-ray binaries may provide a non-negligible contribution to the population of discrete low-luminosity X-ray sources in the Galaxy.

Key words: X-rays: binaries – stars: evolution – stars: neutron – methods: statistical

1 INTRODUCTION

Ongoing deep X-ray surveys of selected Galactic regions have sparked a renewed interest in low-luminosity Galactic X-ray sources such as wind-accreting neutron stars. The XMM–Newton Galactic Plane Survey (e.g. Warwick 2002), the XMM–Newton Serendipitous Survey (Watson 2001; Motch et al. 2002; Motch, Herent & Guillout 2003; Watson et al. 2003) and the serendipitous Chandra Multi-wavelength Plane Survey (Grindlay et al. 2003) will all probe the faint Galactic X-ray point source population.

The discovery by Chandra of more than 500 previously undetected point sources with luminosities above $\simeq 10^{35}$ erg/s in a $2.0^{\circ} \times 0.8^{\circ}$ field near the Galactic centre (Wang, Gottlieb & Lang 2002) dramatically illustrates the potential of such surveys and has already prompted complementing theoretical studies. Pfahl, Rappaport & Podsiadlowski (2002) considered the population of neutron stars that accrete from the wind of an intermediate- or high-mass star (mass $\geq 3 M_{\odot}$). They found that these wind-driven intermediate-mass and high-mass X-ray binaries may indeed account for a dominant fraction of the point source population found by Wang et al. (2002).

Independently, Bleach (2002) investigated the possibility of detecting detached close binaries consisting of a neutron star and a red dwarf, which may be the progenitors of low-mass X-ray binaries (LMXBs). The proposed detection mechanism consists of looking for red dwarfs with X-ray luminosities larger than those expected from intrinsic X-ray

emissions from the star’s corona. The excess could then possibly be ascribed to the emission of X-rays by a neutron star companion accreting mass from the wind of the red dwarf.

Our aim in this paper is to elaborate on the idea by Bleach (2002) and examine the detection probability of pre-LMXBs, i.e. detached neutron-star systems with low-mass companions (mass $\leq 2 M_{\odot}$), in the context of a binary population synthesis study.

2 PRE-LMXBS AND LMXBS

In close binary systems of stars, mass can be transferred from one component to the other when one of the stars loses mass in a stellar wind or when one of the stars fills its Roche lobe. If the companion star is a compact object which is able to accrete some of the transferred mass, the liberation of gravitational potential energy gives rise to an accretion luminosity

$$L_{\text{acc}} = \frac{GM\dot{M}_{\text{acc}}}{R}, \quad (1)$$

where G is the Newtonian constant of gravitation, M and R are the mass and the radius of the accreting compact object, and \dot{M}_{acc} is the mass-accretion rate. We assume that the accretion process yields an X-ray luminosity $L_X \approx L_{\text{acc}}$.

In the particular case of a wind-accreting neutron star, the spin evolution of the neutron star and the possible inhibition of accretion by strong centrifugal forces may play an important role in the study of the accretion process (e.g. Pringle & Rees 1972; Illarionov & Sunyaev 1975; Stella, White, Rosner 1986; Urpin, Geppert & Konenkov 1998).

* E-mail: B.Willems@open.ac.uk, U.C.Kolb@open.ac.uk

The treatment of these inhibiting effects is however beyond the scope of this initial investigation. Instead, we assume that at the onset of mass transfer via the stellar wind, the neutron star’s radiation pressure and rotation rate is low enough for mass accretion to be possible.

The evolution of binaries containing a neutron star is driven by the nuclear evolution of the companion star or by the loss of orbital angular momentum via magnetic braking and/or gravitational radiation. When the combined effect of these processes causes the companion to become larger than its Roche-lobe, an X-ray binary may be formed. The further evolution of the binary depends critically on the orbital period and the mass of the donor star at the onset of Roche-lobe overflow. The formation and evolution of X-ray binaries with low-mass donor stars have been discussed extensively in the past by, e.g., Verbunt (1993); Verbunt & van den Heuvel (1995); Iben & Tutukov (1995); Kalogera & Webbink (1996, 1998); Kalogera (1998); Kalogera, Kolb & King (1998); and more recently by Podsiadlowski, Rappaport & Pfahl (2002). We therefore refer to these studies and references therein for detailed discussions on the various formation channels and here consider the population of X-ray binaries descending from the different channels as a whole.

For the purpose of this investigation, we define a candidate pre-LMXB as a detached binary in which a neutron star accretes mass from the stellar wind of its companion. We assume the latter to be on the main sequence, in the Hertzsprung gap, or on the giant branch, and to have a mass smaller than or equal to $2 M_{\odot}$. The luminosity associated with the accretion process is required to be larger than $10^{-6} L_{\odot}$ or ten times the mass donor’s coronal X-ray luminosity, whichever is larger. We note that our definition of pre-LMXBS differs from that of Bleach (2002) in that we consider stars with masses up to $2 M_{\odot}$ and binaries that are expected to become semi-detached due to the nuclear evolution of the secondary as well as those that are expected to become semi-detached due to angular momentum losses via magnetic braking and/or gravitational radiation.

Similarly, we define a LMXB as a semi-detached system in which a neutron star accretes mass from a Roche-lobe filling main-sequence, Hertzsprung-gap, or giant-branch star with a mass smaller than or equal to $2 M_{\odot}$. In order to be classified as an X-ray binary, we furthermore require the mass-accretion rate to be high enough to produce an X-ray luminosity in excess of $10^{-1} L_{\odot}$.

For the remainder of the paper, we denote the mass and the radius of the neutron star by M_{NS} and R_{NS} , and the mass and the radius of the donor star by M_{d} and R_{d} , respectively.

3 ASSUMPTIONS AND COMPUTATIONAL TECHNIQUE

We explore the possibility of detecting and identifying LMXBs prior to the onset of Roche-lobe overflow from the neutron star’s companion by means of the BiSEPS binary population synthesis code described by Willems & Kolb (2002). The code is based on the analytic approximation formulae for the evolution of single stars derived by Hurley, Pols & Tout (2000) and follows the main lines of the binary evolution algorithm described by Hurley, Tout & Pols

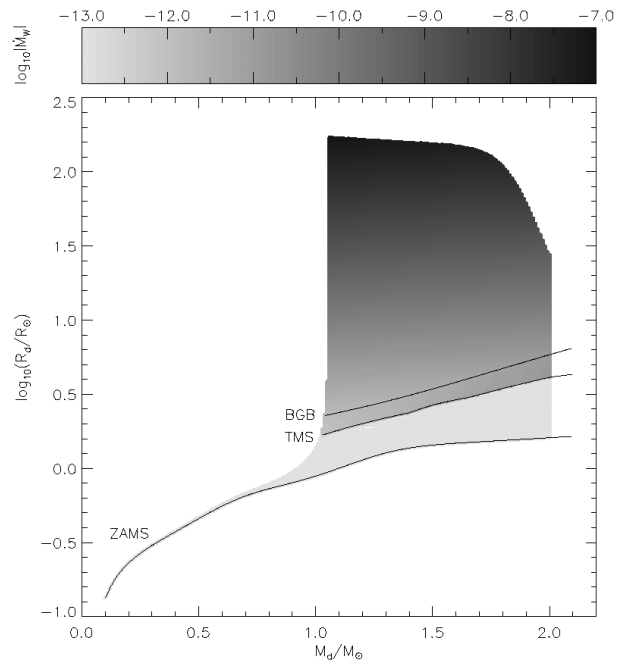


Figure 1. The logarithm of the wind mass-loss rates (in $M_{\odot} \text{ yr}^{-1}$) used in our calculations, as a function of the stellar mass and radius. The lines labelled ZAMS, TMS, and BGB represent the radii of the stars at the zero-age main sequence, the terminal main sequence, and the base of the giant branch, respectively.

(2002). The binary orbits are assumed to be circular and the stellar rotation rates are kept synchronised with the orbital motion at all times. We furthermore restrict ourselves to Population I stellar compositions.

For the purpose of this investigation, the mass-loss rates from stellar winds given by Hurley et al. (2000), which are limited to evolved stars and massive main-sequence stars, must be supplemented by a prescription for the winds from low-mass main-sequence stars. Although these winds are not fully understood yet, it is generally accepted that they depend sensitively on both the mass and the age of the donor star (e.g. Wood et al. 2002, and references therein). Young solar-type stars and M dwarfs, for instance, are thought to have mass-loss rates which may be as high as $10^{-12} M_{\odot}$ per year, while older G dwarfs such as the Sun have mass-loss rates of the order of $10^{-14} M_{\odot}$ per year (Hartmann 1985, Lim & White 1996, van den Oord & Doyle 1997, Wargelin & Drake 2001, Sackmann & Boothroyd 2003). In view of these still existing uncertainties, we here simply adopt a constant mass-loss rate of $10^{-13} M_{\odot}$ per year for low-mass main-sequence stars (see also Bleach 2002). The resulting mass-loss rates are shown in Fig. 1 for donor stars with masses up to $2 M_{\odot}$ and evolutionary stages from the zero-age main sequence up to the tip of the giant branch. The lines labelled ZAMS, TMS, and BGB represent the radii of the stars at the zero-age main sequence, the terminal main sequence, and the base of the giant branch, respectively. The maximum evolutionary age considered for the calculation of the mass-loss rates is 10 Gyr, so that only stars with masses larger than $1 M_{\odot}$ significantly evolve away from the zero-age main sequence.

We estimate the mean mass-accretion rate onto a star orbiting in the stellar wind of its companion by means of a standard Bondi-Hoyle-Lyttleton formalism (Hoyle & Lyttleton 1941, Bondi & Hoyle 1944). The accretion rate for binaries with circular orbits then depends on the orbital separation a , the binary mass ratio q , the donor star's radius R_d , the wind mass-loss rate \dot{M}_d , and the wind velocity v_w . We parametrise the latter as a fraction β_w of the escape velocity $v_e = (2GM_d/R_d)^{1/2}$ at the surface of the mass-losing star (see, e.g., Hurley et al. 2002). The mean wind mass-accretion rate can then be cast in the form

$$\dot{M}_{\text{acc}} = \frac{3}{16} \left(\frac{R_d}{a} \right)^2 \frac{q^2}{\beta_w^4} \left(1 + \frac{1+q}{2} \frac{R_d}{\beta_w^2 a} \right)^{-3/2} |\dot{M}_d|. \quad (2)$$

In the particular case of a wind-accreting neutron star the mass ratio is given by $q = M_{\text{NS}}/M_d$.

The detection mechanism for pre-LMXBs proposed by Bleach (2002) furthermore requires a prescription for the intrinsic X-ray luminosity of the neutron star's companion. Since this luminosity is thought to have its origin in dynamo processes generated by the interaction between convection and rotation, it can be expected to be correlated with the star's rotational angular velocity (e.g. Belvedere, Chiuderi & Paterno 1982; Noyes et al. 1984). The existence of such a correlation was explored extensively from an observational point of view by, e.g., Pallavicini et al. (1981); Marilli & Catalano (1984); Vilhu (1984); Doyle (1987); Fleming, Gioia & Maccacaro (1989); Hempelmann et al. (1995); Randich et al. 1996; Singh et al. (1999); Gondoin (1999). The numerous investigations however show a clear lack of consensus on whether or not the correlation exists and, if it exists, what the precise relationship is between the rotational angular velocity and the coronal X-ray luminosity. This deficiency may be related to the use of different stellar samples and observational selection criteria (Hempelmann et al. 1995, Gondoin 1999).

A point of lesser dispute seems to be the existence of an upper limit on the intrinsic stellar X-ray luminosity, although its origin remains to be unambiguously identified (Walter 1982, Byrne et al. 1984, Vilhu & Walter 1987, Jardine & Unruh 1999, Singh et al. 1999). The upper limit may be related to the finite size of the stellar surface in the sense that the magnetic activity can only increase with increasing rotational angular velocities until the whole stellar surface is covered with magnetically active regions. Based on this idea, Fleming et al. (1989) showed that the coronal saturation luminosity L_{cor} could be related to the square of the stellar radius R_d as

$$\log L_{\text{cor}} = -2.9 + 2 \log R_d, \quad (3)$$

where both L_{cor} and R_d are expressed in solar units (see their Fig. 3).

Rather than face the uncertainties regarding the relation between stellar rotation and coronal X-ray activity, we here opt to use a prescription for the upper limit on the coronal X-ray luminosity. We use the mass of the convective envelope, M_{conv} , to distinguish between coronally active and non-active stars and, somewhat arbitrarily, set the limit for coronal X-ray activity at $M_{\text{conv}} = 0.01 M_d$. Stars with smaller convective envelopes are assumed to have negligible coronal X-ray luminosities, while stars with larger convective envelopes are assumed to have coronal X-ray luminosities

given by Eq. (3). The upper limit may significantly overestimate the coronal X-ray luminosity of giant-type stars with slow rotation rates and correspondingly weak dynamos (Schröder, Hünsch & Schmitt 1998; Gondoin 1999). The slow rotation, however, only applies to giants in wide binaries where tidal forces are negligible. Giants in closer binaries are subjected to tidal torques which tend to synchronise the giant's rotation with the orbital motion of the companion. A significant dynamo action may therefore be sustained in these stars during much more evolved stages of stellar evolution than for single stars or stars in wide binaries. Dempsey et al. (1993, 1997) have shown that in the particular cases of RS Canum Venaticorum (RS CVn) and BY Draconis (BY Dra) binaries the coronal X-ray luminosity of the giant-type component may still reach values up to $0.1 L_{\odot}$. To be on the safe side, we therefore still use the upper limit given by Eq. (3) for stars that have evolved beyond the main-sequence. Where relevant, we will discuss the possible implications of this on our results. In any case, we expect the consistent use of the upper limit for the coronal X-ray luminosity to imply that our selection criteria for the identification of pre-LMXBs are systematically too strict.

4 POPULATION SYNTHESIS

We evolved a large number of binaries with initial component masses ranging from 0.1 to $60 M_{\odot}$ and with initial orbital periods between 0.1 to 10 000 days. We used logarithmically spaced grids consisting of 60 grid points for the initial stellar masses and 200 grid points for the initial orbital periods. The maximum evolutionary age considered was 10 Gyr. If a binary undergoes an asymmetric supernova explosion leading to the birth of a neutron star, 200 random kick velocities are generated from a Maxwellian velocity distribution for the magnitude of the kick velocities. The evolution of the binaries surviving the explosion is then followed until the imposed age limit of 10 Gyr.

The outcome of the binary evolution calculations depends on the parameters adopted for the various evolutionary processes a binary may be subjected to. We therefore vary the input parameters one at a time and compare the resulting populations of pre-LMXBs with that of a reference model. For the latter, hereafter referred to as model A, we adopt the same set of input parameters as in Willems & Kolb (2002), i.e. the common-envelope ejection efficiency parameter takes the value $\alpha_{\text{CE}} = 1.0$, and the Maxwellian kick-velocity dispersion takes the value $\sigma_{\text{kick}} = 190$ km/s. In addition, we here adopt a standard value of 1.0 for the wind-velocity parameter β_w . The different parameters adopted in the other population synthesis models are summarised in Table 1. In the case of the different supernova-kick models, the average kick velocities \bar{v}_{kick} adopted in the Maxwellian velocity distributions are listed in addition to the velocity dispersions σ_{kick} . We also note that the variations in the wind-velocity parameter β_w considered in models MA1 and MA2 are equivalent to considering variations in the wind mass-loss rate \dot{M}_d , but that the parameter β_w is a more appropriate population synthesis parameter since it has a greater impact on the determination of the mean mass-accretion rate. This is readily illustrated by means of Eq. (2) which shows that, to a first approximation, an increase in β_w by a factor of 2

corresponds to a decrease in \dot{M}_d by a factor of the order of 10. Models COR1, COR2, and COR3 are introduced to assess the sensitivity of our results to the prescription for the coronal X-ray luminosity. In particular, the use of a constant value for L_{cor} in models COR1 and COR2 allows us to account for the possible effects of overestimating the coronal X-ray luminosity of giant-type stars by the use of Eq. (3).

The contribution of a system to the population of pre-LMXBs depends on the probability distribution functions of its initial parameters and on the time the system spends as a member of the population. We assume the initial mass M_1 of the primary to be distributed according to the initial mass function

$$\xi(M_1) = \begin{cases} 0 & M_1/M_\odot < 0.1, \\ 0.38415 M_1^{-1} & 0.1 \leq M_1/M_\odot < 0.75, \\ 0.23556 M_1^{-2.7} & 0.75 \leq M_1/M_\odot < \infty, \end{cases} \quad (4)$$

the initial mass ratio $q = M_2/M_1$ according to

$$n(q) = \begin{cases} 1 & 0 < q \leq 1, \\ 0 & q > 1, \end{cases} \quad (5)$$

and the initial orbital separation a according to

$$\chi(a) = \begin{cases} 0 & a/R_\odot < 3 \text{ or } a/R_\odot > 10^4, \\ 0.12328 a^{-1} & 3 \leq a/R_\odot \leq 10^4 \end{cases} \quad (6)$$

(see Willems & Kolb 2002, and references therein).

Each time a binary from our initial grid of parameters evolves into a pre-LMXB, its weighted contribution is added to the probability density function (PDF) describing the distribution of newborn pre-LMXBs in the $(t, M_d, P_{\text{orb}}, L_{\text{acc}})$ -space at the time $t = t_b$ of its formation. The finite lifetime of the pre-LMXBs is taken into account by subtracting the same weighted contribution from the distribution function at the time $t = t_d$ when the system ceases to be a pre-LMXB. In doing so, we implicitly assume that the stellar and orbital parameters of a pre-LMXB do not change significantly once it is formed. We will discuss the circumstances under which this assumption breaks down and the possible implications thereof in the final section of the paper. For now, we remark that this assumption does not affect the determinations of the birthrates and the total number of systems obtained after integration over all system parameters.

The resulting distribution function for the population of pre-LMXBs is subsequently convolved with a constant star-formation rate and normalised so that the integral over all systems found is equal to one.

5 DONOR STAR MASSES AND ORBITAL PERIODS

The normalised distribution function of pre-LMXBs in the $(\log M_d, \log P_{\text{orb}})$ -plane is displayed in Fig. 2 for the most illustrative of the population synthesis models listed in Table 1. Bins containing systems that actually evolve into LMXBs within the imposed age limit of 10 Gyr are outlined with a black solid line.

There are three reasons why systems satisfying our pre-LMXB criteria do not show up in the corresponding LMXB

population. Donor stars with mass $M_d \lesssim 1 M_\odot$ evolve too slowly to fill their Roche lobe as a result of their nuclear evolution within the imposed age limit of 10 Gyr. They can therefore only become LMXBs if their orbital period is shorter than the bifurcation period of ~ 1 day, which separates diverging from converging systems (Pylyser & Savonije 1988, 1989). Donor stars with mass $M_d \gtrsim 1.4 M_\odot$ in systems with $P_{\text{orb}} \gtrsim 2.5$ days on the other hand may fill their Roche lobe when the donor star ascends the first giant branch, but the resulting mass transfer is dynamically unstable so that a common-envelope phase ensues instead of a LMXB phase. Systems with $P_{\text{orb}} \gtrsim 800$ days, finally, are too wide for the donor star to fill its Roche lobe prior to the AGB stage.

The lack of pre-LMXBs in the upper-left corner of each of the plots presented in Fig. 2 is related to our treatment of the coronal X-ray luminosity of the donor stars. Since stars less massive than $\sim 1 M_\odot$ are essentially unevolved and have appreciable convective envelopes, the adopted upper limit for the coronal X-ray luminosity is proportional to the square of the zero-age main sequence radii [Eq. (3)]. The decrease of the latter with decreasing mass then implies that binaries with lower-mass donor stars can satisfy the criterion $L_{\text{acc}} > 10 L_{\text{cor}}$ up to longer orbital periods. The exact position of the lower border of the wedge in the upper-left corner of the figures introduced by this criterion depends on the wind-velocity parameter β_w and on the assumptions made for the determination of the coronal X-ray luminosity L_{cor} . Increasing the wind-velocity parameter (model MA2) yields lower mass-accretion rates and thus lower accretion luminosities. Correspondingly, the bottom of the wedge shifts to lower orbital periods. Adopting a constant upper limit for the coronal X-ray luminosity (models COR1 and COR2, not shown) instead of Eq. (3) renders the border of the wedge introduced by the $L_{\text{acc}} > 10 L_{\text{cor}}$ criterion independent of the mass of the donor star.

Stars more massive than $\sim 1 M_\odot$, on the other hand, may evolve away from the ZAMS within the imposed age limit of 10 Gyr. However, the deep convective envelopes and large radii developed on the giant branch yield high upper limits for the coronal X-ray luminosity so that only few wind-accreting neutron stars manage to top this limit with their accretion luminosity. Most of the pre-LMXBs with $M_d \gtrsim 1 M_\odot$ therefore also have main-sequence donor stars. The rather sharp vertical border of the wedge in the upper-left corner of the figures at $M_d \approx 1 M_\odot$ is then related to the assumed lower limit $M_{\text{conv}} = 0.01 M_d$ for the mass of the convective envelope of coronally active stars. Main-sequence stars more massive than $\sim 1 M_\odot$ have smaller or no convective envelopes and are thus assumed to have negligible coronal X-ray luminosities. The pre-LMXB luminosity criterion therefore reduces to $L_{\text{acc}} > 10^{-6} L_\odot$, which is easily satisfied. If the minimum convective envelope mass necessary for X-ray activity is increased to, e.g., $M_{\text{conv}} = 0.1 M_d$ (model COR3, not shown), the sharp vertical border of the wedge shifts to $M_d \simeq 0.8 M_\odot$.

The group of systems with orbital periods longer than ~ 1000 days and donor star masses between 1.0 and 1.5 M_\odot in the low kick-velocity dispersion models shown in Fig. 2 corresponds to systems with initial orbital separations wide enough to avoid any kind of Roche-lobe overflow prior to the formation of the neutron star. These systems easily survive the supernova explosion of the neutron star's progenitor

Table 1. Population synthesis model parameters.

model	α_{CE}	β_{w}	σ_{kick}	\bar{v}_{kick}	L_{cor}/L_{\odot}	$M_{\text{conv}}/M_{\text{d}}$
A	1.0	1.0	190 km/s	330 km/s	Eq. (3)	0.01
K0	1.0	1.0	no kicks	-	Eq. (3)	0.01
KM25	1.0	1.0	25 km/s	43 km/s	Eq. (3)	0.01
KM50	1.0	1.0	50 km/s	87 km/s	Eq. (3)	0.01
KM75	1.0	1.0	75 km/s	130 km/s	Eq. (3)	0.01
KM100	1.0	1.0	100 km/s	173 km/s	Eq. (3)	0.01
KM300	1.0	1.0	300 km/s	520 km/s	Eq. (3)	0.01
KM400	1.0	1.0	400 km/s	693 km/s	Eq. (3)	0.01
CE1	0.2	1.0	190 km/s	330 km/s	Eq. (3)	0.01
CE2	5.0	1.0	190 km/s	330 km/s	Eq. (3)	0.01
MA1	1.0	0.5	190 km/s	330 km/s	Eq. (3)	0.01
MA2	1.0	2.0	190 km/s	330 km/s	Eq. (3)	0.01
COR1	1.0	1.0	190 km/s	330 km/s	10^{-2} (constant)	0.01
COR2	1.0	1.0	190 km/s	330 km/s	10^{-4} (constant)	0.01
COR3	1.0	1.0	190 km/s	330 km/s	Eq. (3)	0.1

when the average kick velocity is small compared to the relative orbital velocity of the component stars, but generally get disrupted for higher average kick velocities.

The narrow horizontal ridge of systems near $P_{\text{orb}} \approx 10$ days in the low kick-velocity dispersion models ($\sigma_{\text{kick}} \lesssim 100$ km/s) is associated with systems that spiralled-in during a common-envelope phase triggered by Roche-lobe overflow from the neutron star’s progenitor prior to its supernova explosion. The range of orbital periods available for this evolutionary channel is limited by the requirements that the pre-common-envelope orbit must be small enough to initiate Roche-lobe overflow prior to the supernova explosion and wide enough to provide enough orbital energy to expel the common envelope before the core of the Roche-lobe overflowing star merges with the spiralling-in companion. After the expulsion of the envelope, the change in the orbital configuration caused by the supernova explosion depends on the amount of mass lost from the system and on the kick velocity imparted to the neutron star at birth. For a detailed account of the effects of asymmetric supernova explosions on the orbital characteristics of binary stars, we refer to Kalogera (1996).

In the case of small supernova kick-velocity dispersions, the effect of the mass loss dominates over the effect of the kick. The small spread of orbital periods available for the common-envelope scenario is then preserved by the one-to-one relation between the post-supernova orbital period and the mass lost from the system (e.g. Verbunt 1993). Furthermore, since binaries in which more than half of the total mass is lost from the system become unbound after a symmetric supernova explosion, the probability of survival is larger for binaries with more massive donor stars.

In the case of higher supernova kick-velocity dispersions the effect of the kick dominates over the effect of the mass loss. This facilitates the survival of binaries with lower-mass donor stars and increases the spread of the post-supernova orbital periods. The horizontal ridge around $P_{\text{orb}} \approx 10$ days therefore widens and shifts to lower donor star masses.

The common-envelope ejection efficiency parameter α_{CE} only affects systems with orbital periods less than ~ 1000 days. A decrease of α_{CE} (model CE1) yields smaller orbital separations at the end of the common-envelope phase

and thus shifts the horizontal ridge near $P_{\text{orb}} \approx 10$ days to lower orbital periods. This effectively widens the gap between the long- and short-period systems. Increasing the common-envelope efficiency α_{CE} has the opposite effect.

We conclude this section by noting that the position of the high-density areas in Fig. 2 also depends on the adopted initial mass-ratio distribution. Mass ratio distributions favouring lower initial mass ratios (e.g. $n(q) = 1/q$) shift the high-density areas to lower donor star masses, while mass ratio distributions favouring higher initial mass ratios (e.g. $n(q) = q$) shift the high-density areas to higher donor star masses.

6 X-RAY LUMINOSITIES

The normalised distribution functions of pre-LMXBs in the $(\log P_{\text{orb}}, \log L_{\text{acc}})$ - and the $(\log M_{\text{d}}, \log L_{\text{acc}})$ -plane are displayed in Figs. 3 and 4, respectively. Since the qualitative differences between the models listed in Table 1 are small, we limit the figures to models KM50, A, and MA2.

The bulk of the systems shown in Fig. 3 have logarithmic accretion luminosities that are linearly correlated with the logarithm of the orbital period. The slope of $-4/3$ arises from Kepler’s third law and the factor $1/a^2$ in Eq. (2) for the mean mass-accretion rate \dot{M}_{acc} . Since most of the systems following the correlation have main-sequence donor stars, the small spread around the correlation is the result of the limited range of donor star masses and radii and the adopted constant wind mass-loss rate of $10^{-13} M_{\odot}$ per year [see Eq. (2)]. In the case of low supernova kick-velocity dispersions, the two distinct higher-density regions along the $L_{\text{acc}} \propto P_{\text{orb}}^{-4/3}$ relation correspond to the two groups of systems identified in the low kick-velocity dispersion models shown in Fig. 2. The high accretion luminosities around 10^{31} erg/s stem from systems on the horizontal ridge around $P_{\text{orb}} \approx 10$ days, while the lower accretion luminosities around 10^{28} erg/s stem from the long-period systems with $P_{\text{orb}} \gtrsim 1000$ days. For higher kick-velocity dispersions, only the first group of systems survives. The accretion luminosities of the pre-LMXBs on the $L_{\text{acc}} \propto P_{\text{orb}}^{-4/3}$ furthermore decrease with increasing values of the wind-velocity parameter β_{w} .

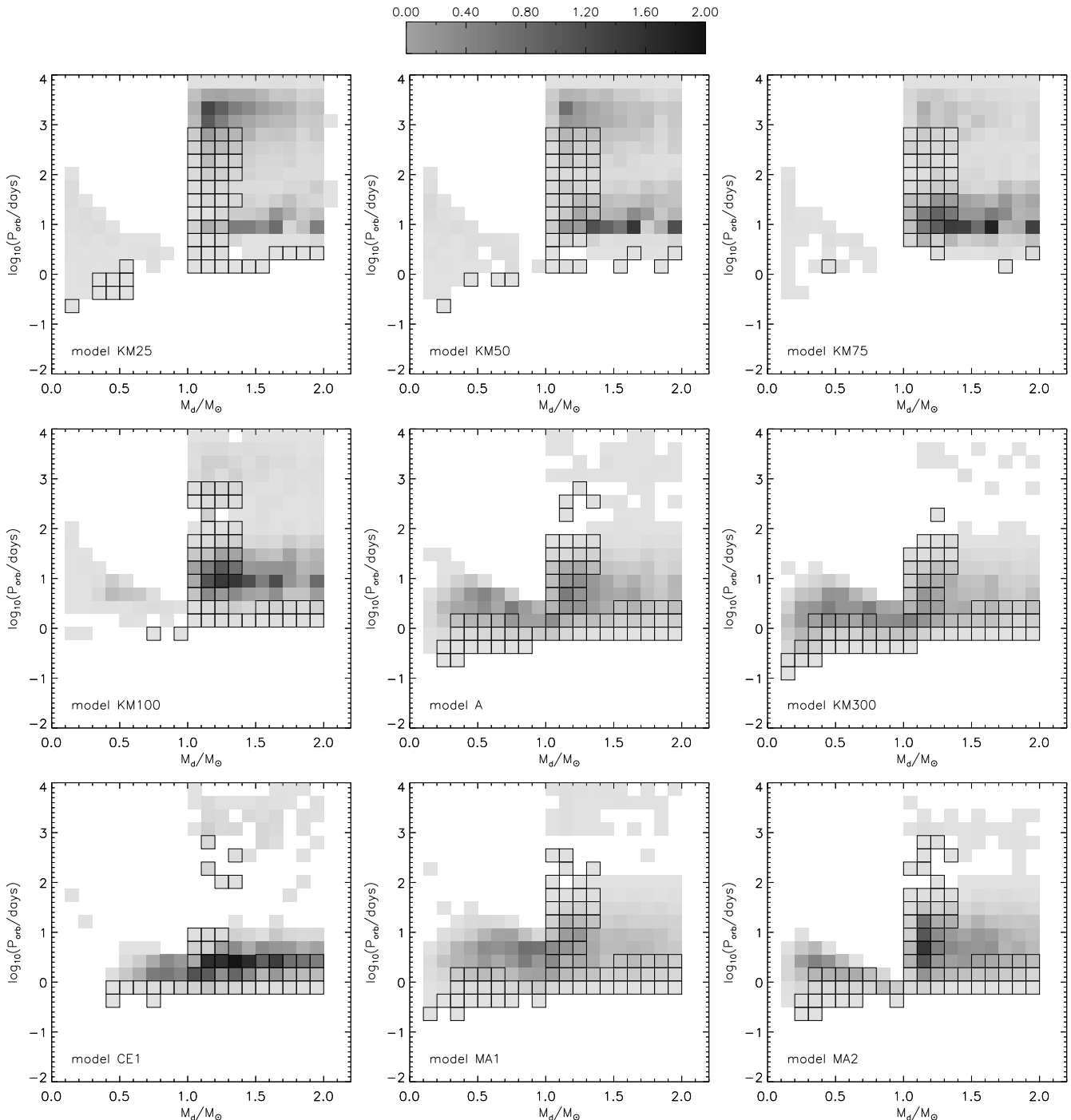


Figure 2. Normalised distribution of pre-LMXBs in the $(\log M_d, \log P_{\text{orb}})$ -plane. The outlined boxes correspond to bins containing pre-LMXBs which actually evolve into LMXBs within the imposed age limit of 10 Gyr.

The branch of systems located to the right of the $L_{\text{acc}} \propto P_{\text{orb}}^{-4/3}$ correlation corresponds to pre-LMXBs with giant branch donor stars. Most of these already appeared as pre-LMXBs when the donor star was still on the main-sequence, but the growth of the convective envelope and the associated increase in the coronal X-ray activity during the post-main-sequence evolution temporarily concealed the X-ray accretion luminosity emitted by the wind-accreting neutron star. The functional form of the mean mass-accretion rate \dot{M}_{acc} [Eq. (2)] implies that systems with longer orbital

periods require more evolved donor stars, i.e. stars with larger radii and higher wind mass-loss rates, to satisfy the imposed $L_{\text{acc}} > 10 L_{\text{cor}}$ criterion. However, the larger radii in turn imply a larger upper limit for the coronal X-ray luminosity L_{cor} [Eq. (3)], so that at the time of reappearance the $10 L_{\text{cor}}$ threshold itself will be higher for systems with wider orbital separations. Hence, the accretion luminosity at which the systems reappear as pre-LMXBs increases with increasing orbital periods. Their reappearance also de-

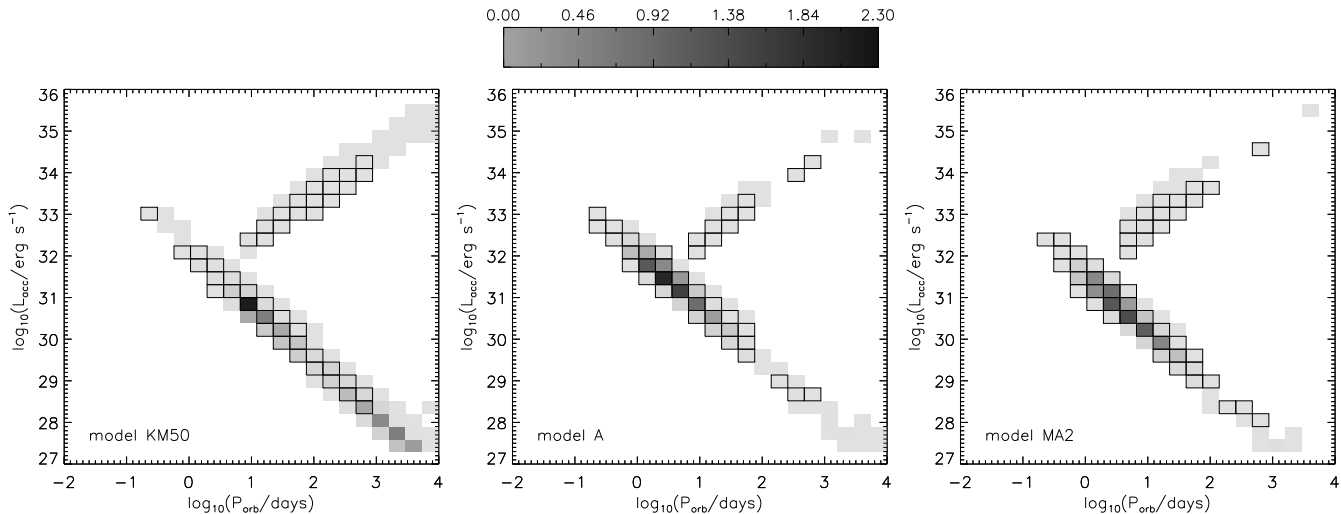


Figure 3. Normalised distribution of pre-LMXBs in the $(\log P_{\text{orb}}, \log L_{\text{acc}})$ -plane. The outlined boxes correspond to bins containing pre-LMXBs which actually evolve into LMXBs within the imposed age limit of 10 Gyr.

depends critically on whether or not the accretion luminosity increases faster than the coronal X-ray luminosity.

The position of the giant-branch stars in the $(\log P_{\text{orb}}, \log L_{\text{acc}})$ -plane clearly depends on the assumptions adopted for the determination of L_{acc} and L_{cor} . Since higher wind velocities yield lower mass-accretion rates, an increase in the wind-velocity parameter β_w as in model MA2 requires even more evolved donor stars to satisfy the $L_{\text{acc}} > 10 L_{\text{cor}}$ criterion than in model A. The reappearance threshold of these systems consequently moves to higher accretion luminosities. In the case of a constant coronal X-ray luminosity (models COR1 and COR2, not shown), the accretion luminosity at which systems with giant branch donor stars reappear as pre-LMXBs is independent of the orbital period. The temporary concealment of the accretion luminosity probably does not occur for the longer period systems ($P_{\text{orb}} \gtrsim 100$ days) in which tidal forces are too weak to keep the donor star’s rotation synchronised with the orbital motion of the companion. The decrease of the donor star’s rotational angular velocity during its post-main-sequence evolution is here more likely to be accompanied by a decrease in the coronal X-ray activity so that the wind-accretion luminosity in these binaries has no problem topping the coronal X-ray luminosity at any time after they first appear as a pre-LMXB.

The linear correlation between $\log L_{\text{acc}}$ and $\log P_{\text{orb}}$ for the bulk of the systems presented in Fig. 3 essentially makes Fig. 4 a mirror image of Fig. 2. The low kick-velocity dispersion models hence again show two distinct groups of systems at high and low accretion luminosities, which are associated with the horizontal ridge and the long-period systems observed in Fig. 2. In our standard model (model A), even systems with donor stars less massive than $1.0 M_{\odot}$ are seen to give rise to accretion luminosities up to 10^{32} erg/s. An increase in the wind-velocity parameter β_w shifts all systems to lower accretion luminosities.

Finally, the one-dimensional distribution functions of the pre-LMXB accretion luminosities are presented in Fig. 5 for the same population synthesis models as in Fig. 2. We distinguish between systems that actually evolve into LMXBs within the imposed age limit of 10 Gyr and those

that do not by means of light and dark grey shadings, respectively. The distribution of pre-LMXB accretion luminosities in our standard population synthesis model shows a primary peak around 10^{31} erg/s and a small secondary peak around 10^{28} erg/s. The latter becomes more important with decreasing kick-velocity dispersions and dominates when $\sigma_{\text{kick}} = 25$ km/s. This shift towards lower accretion luminosities is related to the increasing contribution of the long-period systems with $P_{\text{orb}} \gtrsim 1000$ days. The width of the peak at 10^{31} erg/s depends primarily on the common-envelope ejection efficiency parameter α_{CE} . The peak becomes narrower with decreasing values of α_{CE} due to the shrinking range of post-supernova orbital periods around $P_{\text{orb}} \approx 10$ days. Increasing the wind-velocity parameter β_w moves the distribution function to lower X-ray luminosities, while a decrease in β_w has the opposite effect. A similar tendency was found by Pfahl et al. (2002). It is also interesting to note that the peak luminosity of 10^{31} erg/s is comparable to the luminosity originating from non-magnetic white dwarfs accreting mass from a Roche-lobe filling companion (cataclysmic variables). Such systems may be distinguishable from pre-LMXBs based on the harder X-ray spectrum expected for wind-accreting neutron stars. In addition, white dwarfs can possibly be detected in the optical or UV wavelengths, provided that they are bright enough.

7 RELATIVE AND ABSOLUTE NUMBER OF PRE-LMXBS IN THE GALAXY

The relative number of pre-LMXBs evolving into LMXBs within the imposed age limit of 10 Gyr are listed in the first column of Table 2. In general, about 20 to 30 per cent of all systems satisfying our pre-LMXB criteria evolve into a LMXB in a time span of less than 10 Gyr. This fraction decreases significantly for kick-velocity dispersions smaller than ~ 50 km/s (model KM50) due to the growing contribution of systems with orbital periods longer than ~ 1000 days. A decrease of the common-envelope efficiency parameter α_{CE} (model CE1) on the other hand increases the relative

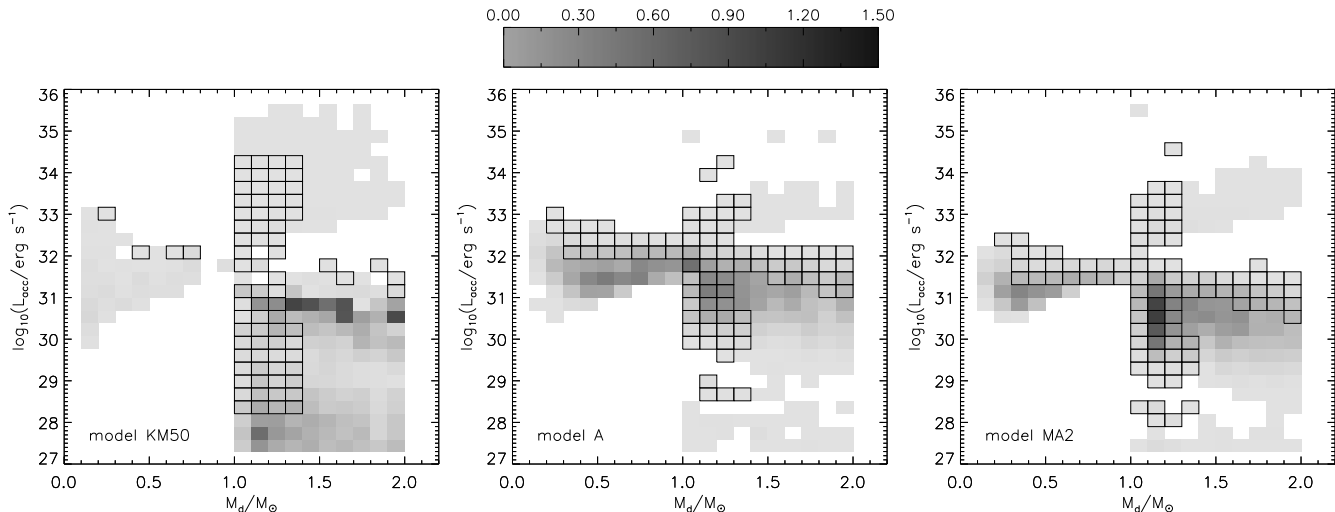


Figure 4. Normalised distribution of pre-LMXBs in the $(\log M_d, \log L_{acc})$ -plane. The outlined boxes correspond to bins containing pre-LMXBs which actually evolve into LMXBs within the imposed age limit of 10 Gyr.

Table 2. Relative number of pre-LMXBs evolving into LMXBs within the imposed age limit of 10 Gyr and relative number of LMXBs descending from a pre-LMXB.

model	pre-LMXBs evolving into LMXBs	LMXBs descending from pre-LMXBs
A	31.9%	43.5%
K0	21.3%	0.1%
KM25	12.7%	14.3%
KM50	16.1%	10.8%
KM75	24.1%	8.5%
KM100	28.7%	9.7%
KM300	30.1%	48.7%
KM400	29.5%	48.2%
CE1	40.7%	14.9%
CE2	33.2%	73.6%
MA1	26.1%	36.9%
MA2	41.2%	39.1%
COR1	45.8%	43.2%
COR2	24.7%	43.5%
COR3	26.5%	43.5%

number of pre-LMXBs evolving into LMXBs since it boosts the contribution of the short-period systems. Similarly, increasing the wind-velocity parameter β_w (model MA2) decreases the accretion luminosities of the longer period systems below the $L_{acc} > 10 L_{cor}$ threshold so that again the relative number of pre-LMXBs evolving into LMXBs increases. If Eq. (3) is replaced by a constant coronal X-ray luminosity of $10^{-2} L_{\odot}$ (model COR1), a large fraction of the low-mass systems with $M_d \lesssim 1 M_{\odot}$ can no longer satisfy the $L_{acc} > 10 L_{cor}$ criterion. The disappearance of these systems causes an increase of the relative number of pre-LMXBs that will evolve into LMXBs.

Although a detailed population synthesis study of the formation and evolution of LMXBs is beyond the scope of this investigation, it is interesting to consider the relative number of LMXBs that are expected to evolve through a phase satisfying our pre-LMXB criteria. The relative numbers are listed in the second column of Table 2 and typically

range 30 to 50 per cent. The LMXBs that did not evolve through a pre-LMXB phase all descend from intermediate mass X-ray binaries (IMXB) with initial donor star masses outside the mass range considered in this investigation (see also King & Ritter 1999; Podsiadlowski & Rappaport 2000; Kolb et al. 2000; Pfahl, Rappaport & Podsiadlowski 2003). A substantial fraction of LMXBs thus evolves through an X-ray bright wind-accretion phase prior to the onset of Roche-lobe overflow from the neutron star’s companion.

For conclusion, we estimate the order of magnitude of the birthrate and the absolute number of pre-LMXBs currently populating the Galaxy. To this end, we assume all stars to be in binaries and we normalise the star formation rate to produce a Galactic type II supernova rate of 10^{-2} per year (Cappellaro, Evans & Turatto 1999). The resulting birthrates and absolute numbers are listed in Table 3. Based on these calculations, we expect the current population of pre-LMXBs in the Galactic disk to exist of about 10^4 – 10^5 systems, so that they may account for a non-negligible part of the X-ray output in large scale surveys performed by Chandra and XMM.

8 DISCUSSION

We have investigated the population of candidate pre-low-mass X-ray binaries according to the detection mechanism proposed by Bleach (2002). The mechanism is based on the search for low-mass stars with X-ray luminosities that are too large to be attributed to the stellar coronal activity, and on the subsequent identification of neutron star binaries amongst these stars. The X-ray excess in these binaries can then possibly be ascribed to the accretion of mass by the neutron star from the stellar wind of its companion.

In our study, we used the BiSEPS binary population synthesis code described by Willems & Kolb (2002). We limited ourselves to neutron star binaries with main-sequence, Hertzsprung-gap, or giant-branch donor stars of mass $M_d \lesssim 2 M_{\odot}$ and simulated the X-ray excess by the requirement that the X-ray luminosity generated by the wind-

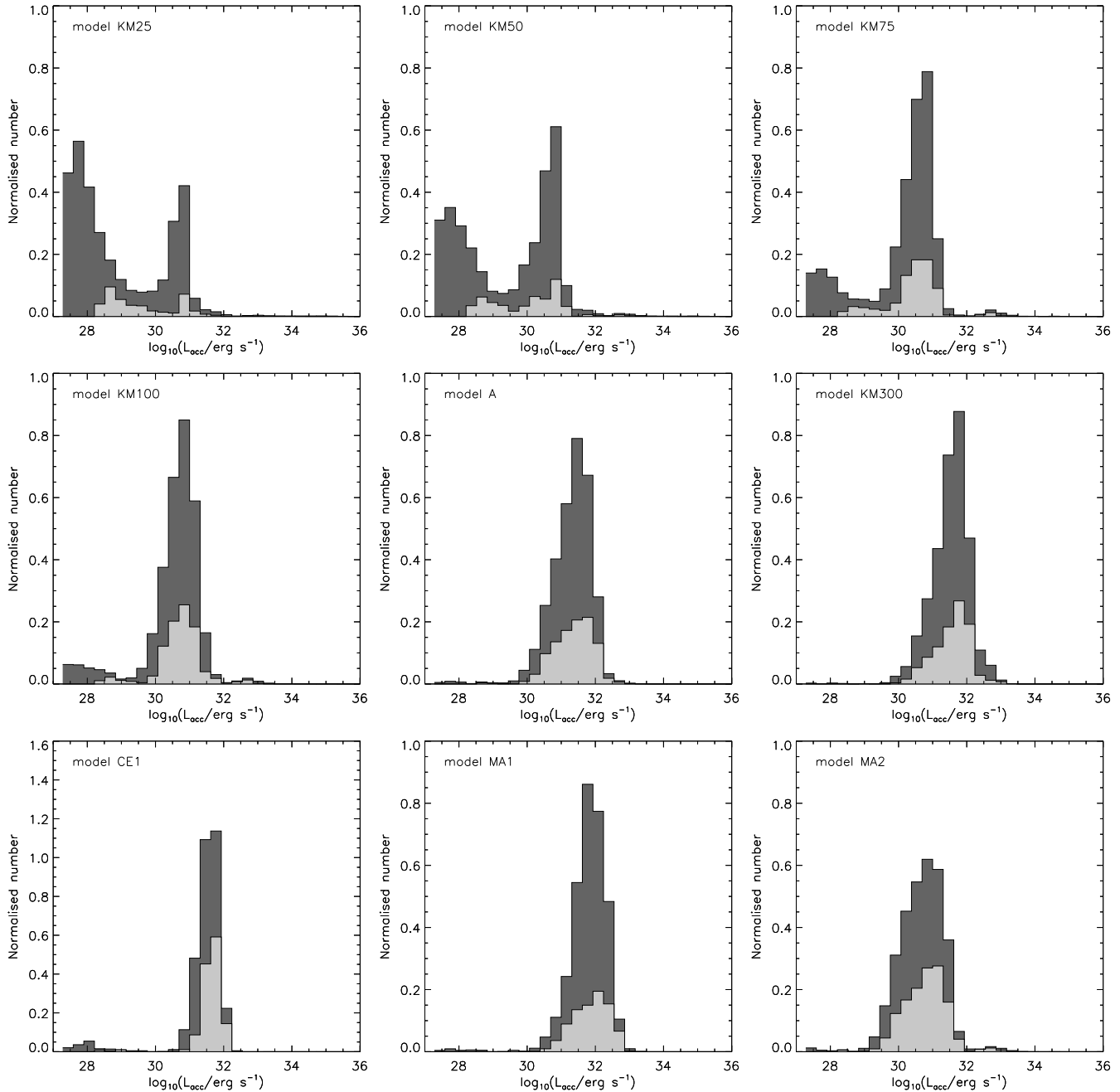


Figure 5. Normalised distribution functions of pre-LMXB accretion luminosities. Light and dark grey shadings correspond to the contributions of systems that do and do not evolve into LMXBs within the imposed age limit of 10 Gyr, respectively.

accreting neutron star be at least 10 times larger than the coronal X-ray luminosity of the mass-losing star. The X-ray luminosity associated with the accretion process was determined under the assumptions that no accretion-inhibiting effects such as strong centrifugal forces are present and that all gravitational potential energy of the infalling matter is converted into X-ray radiation. The maximum coronal X-ray luminosity for a star of a given mass and radius was assumed to be proportional to the square of the star's radius.

It follows that, in the case of low supernova kick-velocity dispersions, the population of pre-LMXBs can be

divided into two groups of systems: a long-period group with $P_{\text{orb}} \gtrsim 1000$ days and a short-period group with $P_{\text{orb}} \approx 10$ days. The division yields a bimodal distribution for the accretion luminosities of the candidate pre-LMXBs. The long-period systems produce a peak in the distribution around 10^{28} erg/s, while the short-period systems produce a peak near 10^{31} erg/s. For kick-velocity dispersions larger than ~ 100 km/s only the peak near 10^{31} erg/s remains. The luminosity at which the distribution peaks furthermore depends sensitively on the velocity of the donor star's wind.

These results are derived under the assumption that the stellar and orbital parameters, and in particular the orbital

Table 3. Birthrates and total number of Galactic pre-LMXBs for each of the population synthesis models listed in Table 1. The models are normalised to a Galactic type II supernova rate of 10^{-2} per year.

model	birthrate (yr^{-1})	total number
A	2.1×10^{-6}	5.0×10^4
K0	1.6×10^{-7}	7.9×10^4
KM25	3.9×10^{-7}	6.5×10^4
KM50	2.7×10^{-7}	4.3×10^4
KM75	2.3×10^{-7}	3.3×10^4
KM100	4.3×10^{-7}	3.6×10^4
KM300	1.9×10^{-6}	3.7×10^4
KM400	1.2×10^{-6}	2.3×10^4
CE1	2.4×10^{-7}	1.2×10^4
CE2	7.5×10^{-6}	2.0×10^5
MA1	3.3×10^{-6}	6.5×10^4
MA2	8.5×10^{-7}	4.0×10^4
COR1	3.2×10^{-7}	3.2×10^4
COR2	3.8×10^{-6}	7.0×10^4
COR3	3.3×10^{-6}	6.5×10^4

period and the accretion luminosity, of pre-LMXBs remain unchanged after their formation. This assumption breaks down for binaries with $M_d \lesssim 1 M_\odot$ and $P_{\text{orb}} \lesssim 1$ day in which the evolution is governed by the loss of angular momentum via gravitational radiation and/or magnetic braking, and for binaries with $M_d \gtrsim 1 M_\odot$ in which the evolution is governed by the nuclear evolution of the donor star.

First, the decrease of the orbital period resulting from the angular momentum loss in binaries with $M_d \lesssim 1 M_\odot$ and $P_{\text{orb}} \lesssim 1$ day yields an increase of the mean mass-accretion rate and thus of the accretion luminosity generated by the neutron star. However, from Eqs. (1) and (2) it follows that an increase of the accretion luminosity by a factor of 10 requires a decrease of the orbital period by a factor of ~ 5.6 . For a pre-LMXB with an orbital period of ~ 1 day, this comes down to a decrease of the period to ~ 4.3 hours. Since neutron star binaries with secondaries more massive than $\sim 0.5 M_\odot$ becomes semi-detached before they can reach such short periods, we can expect that the neglect of the orbital evolution does not affect our estimates for the accretion luminosities by more than an order of magnitude.

Second, the nuclear evolution of donor stars more massive than $\sim 1 M_\odot$ may yield a significant increase of the star's radius and wind mass-loss rate within the age of the Galaxy. The effect of both these evolutionary aspects is to increase the mean mass-accretion rate of the neutron star. However, for main-sequence stars less massive than $2 M_\odot$, the increase of the stellar radius increases the mean mass-accretion rate by less than an order of magnitude [see Eqs. (1) and (2)]. The overall effect on our results can therefore again be expected to be small. The main uncertainty for main-sequence donor stars consequently stems from their poorly understood wind mass-loss rates (e.g. Wargelin & Drake 2001). Pre-LMXBs with donor stars that have evolved beyond the main-sequence, on the other hand, have better understood mass-loss rates, but contribute too little to the total population of newborn pre-LMXBs to have a significant effect on the distribution functions presented. In addition, systems with an orbital period of the order of a few days will evolve into LMXBs shortly after the secondary

leaves the main sequence. A significant increase in the X-ray accretion luminosity is therefore only possible for wider systems which do not initiate Roche-lobe overflow until the secondary is well on its way towards the tip of the giant branch or for systems which do not initiate Roche-lobe overflow at all. For these systems, we may underestimate the maximum accretion luminosity by several orders of magnitude, but since the life time of a star on the giant branch is much shorter than its main sequence life time, the contribution of the systems to the pre-LMXB population during this phase is smaller than their contribution when the donor star was still on the main sequence. In addition, the wider orbital separations required for this scenario somewhat counteract the increase in the accretion luminosity associated with the evolution of the donor star.

Finally, we estimated the total number of pre-LMXBs currently populating the Galaxy to be of the order of 10^4 – 10^5 . For comparison, the estimated number of RS CVn type binaries in the Galaxy is of the order of 10^6 (Watson 1990) and the theoretically predicted number of cataclysmic variables in the Galaxy is of the order of 10^6 – 10^7 (Kolb & Willems 2003, in preparation). Both these types of systems have X-ray luminosities comparable to the 10^{31} erg/s peak luminosity found in our models for candidate pre-LMXBs. In addition, the distribution of X-ray luminosities at 10^{28} erg/s may be expected to be dominated by coronally active stars. Our predicted number of pre-LMXBs satisfying the X-ray excess criterion is therefore small in comparison to the number of these other low-luminosity X-ray sources, but nevertheless high enough to possibly account for an interesting fraction of the low-luminosity discrete X-ray sources observed by Chandra and XMM. A systematic search for candidate pre-LMXBs based on the X-ray excess criterion can in principle be initiated by comparing existing X-ray (ROSAT, Einstein, Chandra and XMM) and optical (Hipparcos, Tycho, HST GSC) source catalogs. Simultaneous X-ray and optical observations by XMM provide an attractive alternative.

ACKNOWLEDGEMENTS

We thank Jarrod Hurley, Onno Pols, and Chris Tout for sharing their SSE software package; and Philipp Podsiadlowski, Firoza Sutaria and Robin Barnard for useful discussions. The referee, Peter Wheatley, is thanked for his constructive remarks. This research was supported by the British Particle Physics and Astronomy Research Council (PPARC).

REFERENCES

- Belvedere G., Chiuderi C., Paterno L., 1982, A&A 105, 133
- Bleach J.N., 2002, MNRAS 332, 689
- Bondi H., Hoyle F., 1944, MNRAS 104, 273
- Byrne P.B., Doyle J.G., Butler C.J., Andrews, A.D., 1984, MNRAS 211, 607
- Cappellaro E., Evans R., Turatto M., 1999, A&A 351, 459
- Dempsey R.C., Linsky J.L., Fleming T.A., Schmitt J.H.M.M., 1993, ApJS 86, 599
- Dempsey R.C., Linsky J.L., Fleming T.A., Schmitt J.H.M.M., 1997, ApJ 478, 358

- Doyle J.G., 1987, MNRAS 224, 1P
- Fleming T.A., Gioia I.M., Maccacaro T., 1989, ApJ 340, 1011
- Gondoin P., 1999, A&A 352, 217
- Grindlay J., Zhao O., Hong J., Jenkins J., Kim D.-W., Schlegel E., Drake J., Kashyap V., Edmonds P., Cohn H., Lugger P., Cool A., 2003, in X-ray Surveys in the light of the new observatories, Astron. Nachr. 324, 57
- Hartmann L., 1985, Solar Physics 100, 587
- Hempelmann A., Schmitt J.H.M.M., Schultz M., Ruediger G., Stepien K., 1995, A&A 294, 515
- Hoyle F., Lyttleton R.A., 1941, MNRAS 101, 227
- Hurley J.R., Pols O.R., Tout C.A., 2000, MNRAS 315, 543
- Hurley J.R., Tout C.A., Pols O.R., 2002, MNRAS 329, 897
- Iben I. Jr., Tutukov A.V., 1995, in Millisecond Pulsars: A Decade of Surprise, Eds. A.S. Fruchter, M. Tavani, D.C. Backer, ASP Conference Series 72, 119
- Illarionov A.F., Sunyaev R.A., 1975, A&A 39, 185
- Jardine M., Unruh Y.C., 1999, A&A 346, 883
- Kalogera V., 1996, ApJ 471, 352
- Kalogera V., Webbink R.F., 1996, ApJ 458, 301
- Kalogera V., Webbink R.F., 1998, ApJ 493, 351
- Kalogera V., 1998, ApJ 493, 368
- Kalogera V., Kolb U., King A.R., 1998, ApJ 504, 967
- King A.R., Ritter H., 1999, MNRAS 309, 253
- Kolb U., Davies M.B., King A., Ritter H., 2000, MNRAS 317, 438
- Kolb U., Willems B., 2003, in preparation
- Lim J., White S.M., 1996, ApJ 462, L91
- Marilli E., Catalano S., 1984, A&A 133, 57
- Motch C., et al., 2002, ESA SP-488 (astro-ph/0203025)
- Motch C., Herent O., Guillout P., 2003, in X-ray Surveys in the light of the new observatories, Astron. Nachr. 324, 61
- Noyes R.W., Hartmann L.W., Baliunas S.L., Duncan D.K., Vaughan A.H., 1984, ApJ 279, 763
- Pallavicini R., Golub L., Rosner R., Vaiana G.S., Ayres T., Linsky J.L., 1981, ApJ 248, 279
- Pfahl E.D., Rappaport S., Podsiadlowski P., 2002, ApJ 571, L37
- Pfahl E.D., Rappaport S., Podsiadlowski P., 2003, ApJ, submitted (astro-ph/0303300)
- Podsiadlowski P., Rappaport S., 2000, ApJ 529, 946
- Podsiadlowski P., Rappaport S., Pfahl E.D., 2002, ApJ 565, 1107
- Pringle J.E., Rees M.J., 1972, A&A 21, 1
- Pylyser E., Savonije G.J., 1988, A&A 191, 57
- Pylyser E., Savonije G.J., 1989, A&A 208, 52
- Randich S., Schmitt J.H.M.M., Prosser C.F., Stauffer J.R., 1996, A&A 305, 785
- Sackmann I.-J., Boothroyd A.I., 2003, ApJ 583, 1024
- Schröder K.-P., Hünsch M., Schmitt J.H.M.M., 1998, A&A 335, 591
- Singh K.P., Drake S.A., Gotthelf E.V., White N.E., 1999, ApJ 512, 874
- Stella L., White N.E., Rosner R., 1986, ApJ 308, 669
- Urpin V., Geppert U., Kononov D., 1998, MNRAS 295, 907
- van den Oord G.H.J., Doyle J.G., 1997, A&A 319, 578
- Verbunt F., 1993, ARA&A 31, 93
- Verbunt F., van den Heuvel E.P.J., 1995, in X-ray Binaries, Eds. Lewin W.H.G., van Paradijs J., van den Heuvel E.P.J., Cambridge University Press, Cambridge
- Vilhu O., 1984, A&A 133, 117
- Vilhu O., Walter F.M., 1987, ApJ 321, 958
- Walter F.M., 1982, ApJ 253, 745
- Wang Q.D., Gotthelf E.V., Lang C.C., 2002, Nature 415, 148
- Wargelin B.J., Drake J.J., 2001, ApJ 546, L57
- Warwick R.S., 2002, ESA SP-44 (astro-ph/0203333)
- Watson M.G., 1990, in Windows on Galaxies, Eds. Fabbiano G., Gallagher J.S., Renzini A., Kluwer, Dordrecht, 177
- Watson M.G., 2001, A&A 365, L51
- Watson M.G., Pye J.P., Denby M., Osborne J.P., Barret D., Boller Th., Brunner H., Ceballos M.T., DellaCeca R., Fyfe D.J., Lamer G., Maccacaro T., Michel L., Motch C., Pietsch W.N., Saxton R.D., Schroeder A.C., Stewart I.M., Tedds J.A., Webb N., 2003, in X-ray Surveys in the light of the new observatories, Astron. Nachr. 324, 89
- Willems B., Kolb U., 2002, MNRAS 337, 1004
- Wood B.E., Müller H.-R., Zank G.P., Linsky J.L., 2002, ApJ 574, 412

This paper has been typeset from a \TeX / \LaTeX file prepared by the author.